Live-cell photoactivated localization microscopy of nanoscale adhesion dynamics

Hari Shroff, Catherine G Galbraith, James A Galbraith & Eric Betzig

Supplementary figures and text:

Note: Supplementary Videos 1–9 are available on the Nature Methods website.

Supplementary Figure 1

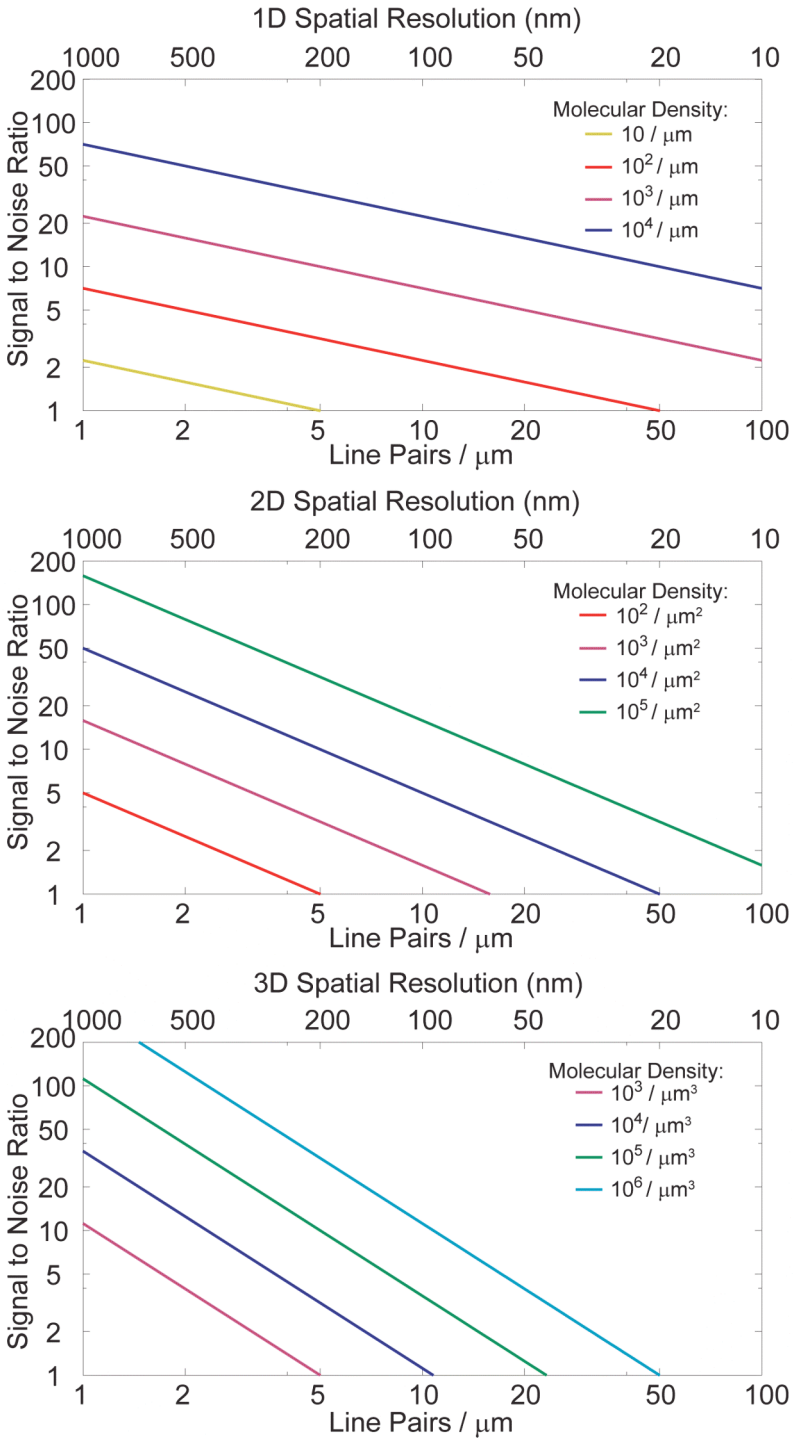

Dependence of signal-to-noise ratio (SNR) on resolution and molecular density.

Log-log plots of SNR due to stochastic variations in the number of molecules per pixel, as a function of resolution and molecular density in 1 (top), 2 (middle), or 3 (bottom) dimensions. The requisite molecular density increases as the desired SNR increases, or as the dimensionality increases.

Supplementary Figure 2

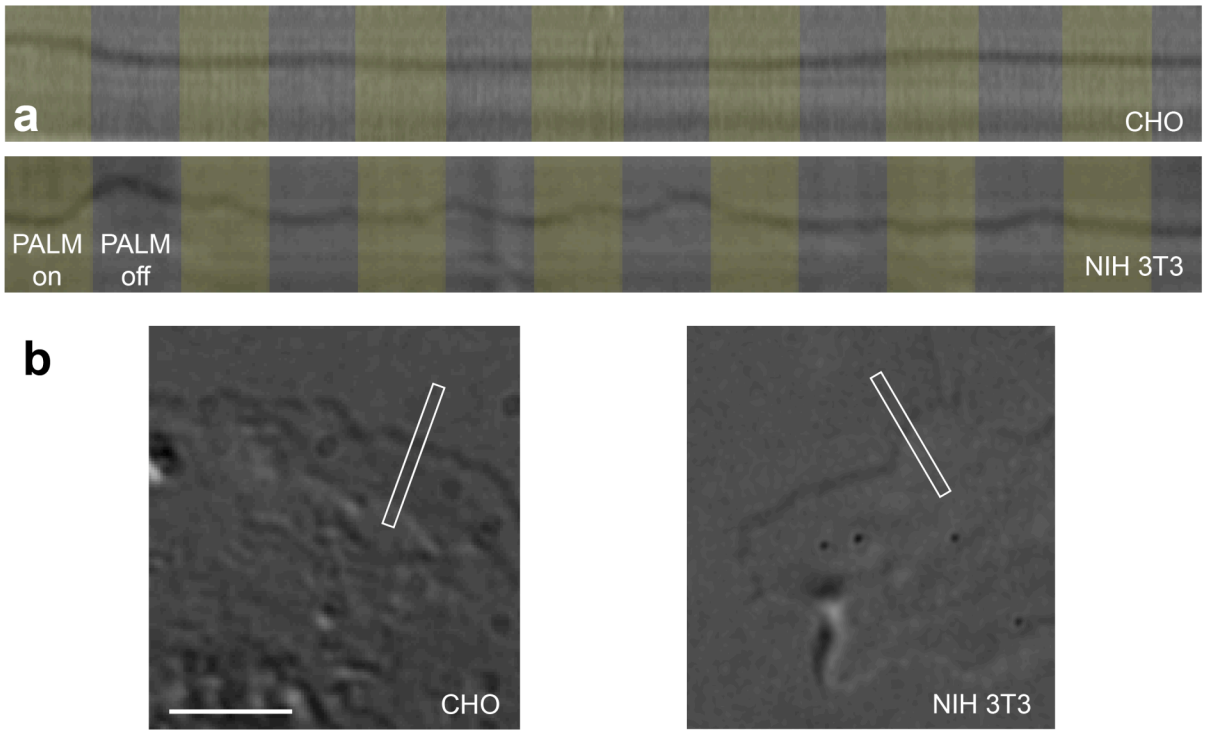

Cell protrusive activity is unaffected by PALM acquisition. DIC images were collected continuously every 2 seconds while PALM acquisition was cycled on (yellow bands) and off (gray bands) every 60 s. (**a**) Kymograph of leading edge for CHO and NIH 3T3 cells. (**b**) DIC images of CHO (left) and NIH 3T3 (right) cells with box indicating region used to generate kymograph. Scale bar, 5 μm.

Supplementary Figure 3

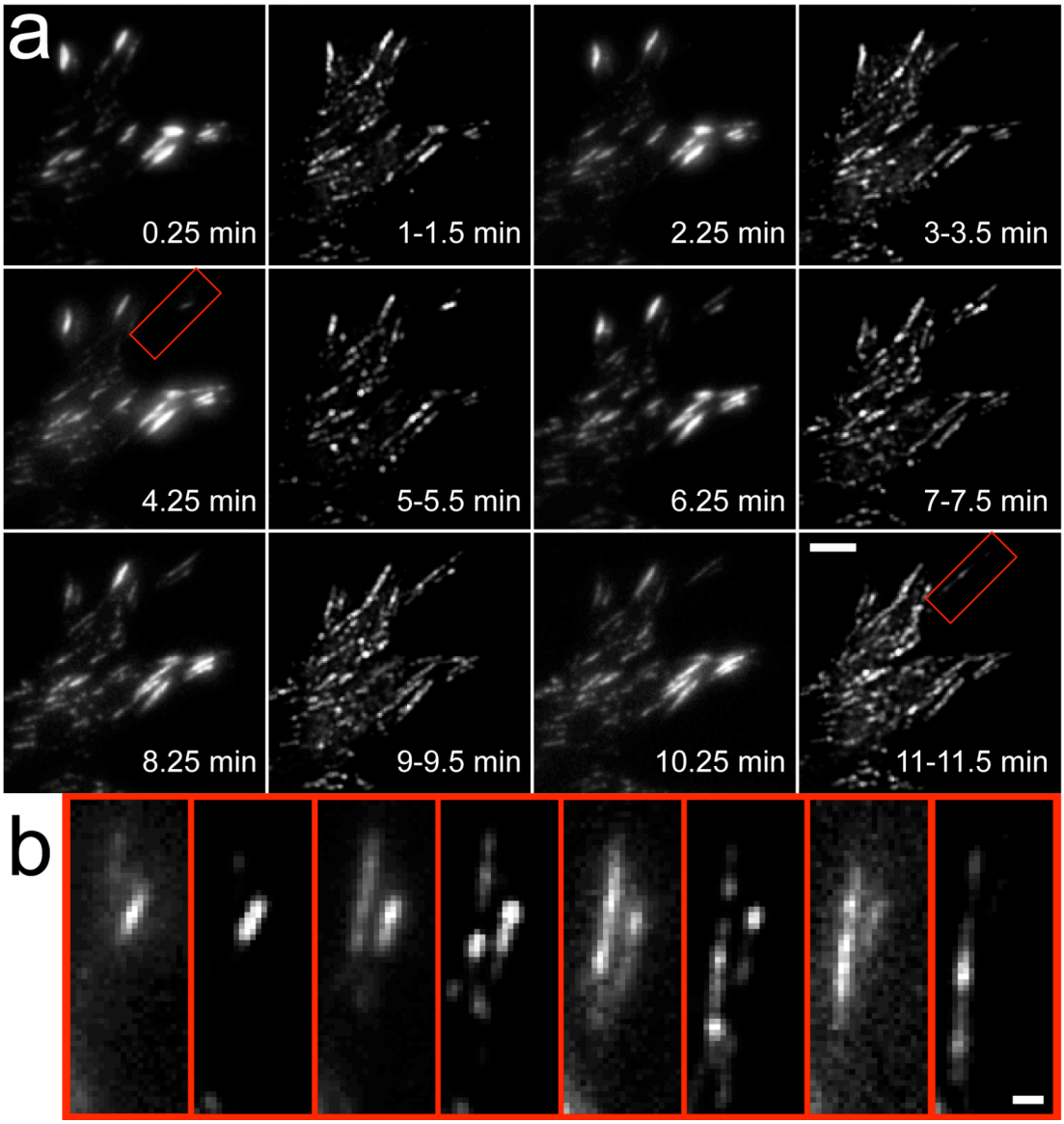

AC dynamics under PALM conditions are similar to those under low intensity diffraction-limited imaging.
An NIH 3T3 cell expressing tdEos/paxillin was alternately excited with low (~0.001 kW/cm^2) 488 nm intensity and the much higher (1 kW/cm^2) 561 nm and 405 nm (0.05 kW/cm^2) intensities used in PALM-imaging. (**a**) Alternating diffraction-limited TIRF (via 488 nm illumination) and summed TIRF (via 561 nm, 405 nm illumination) images. Summed TIRF images recapitulate ACs evident in the diffraction-limited images, indicating that morphology is preserved at the intensities used in PALM. The summed TIRF images are derived from analyzed PALM data, and thus show more detail and lower background than diffraction-limited images. (**b**) Higher magnification view of the AC in frames 5-12 (red box in (**a**)), showing elongation as a function of time. Scale bars: 5 m (**a**), 1 m (**b**).

Supplementary Figure 4

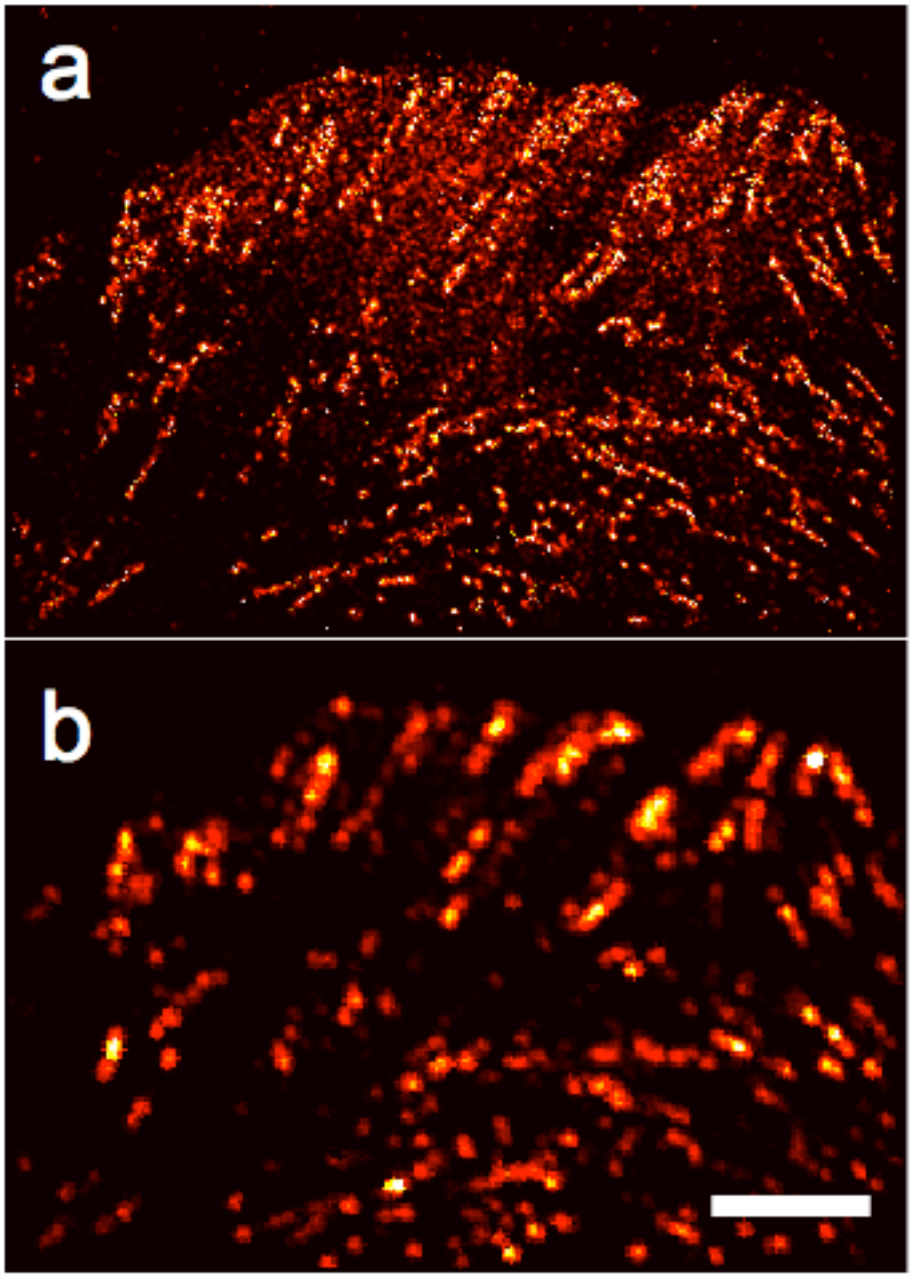

Range of molecular density visible by PALM vs. summed TIRF. (**a**) Single frame from live cell PALM time series of a CHO cell transfected with tdEos/paxillin. In addition to adhesion complexes, a large pool of dissociated paxillin is present near the cell edge. (**b**) Summed TIRF image of data plotted in (**a**). The same pool of paxillin is invisible when adhesion complexes are not plotted at saturating intensities. Images were composed from 625 single molecule frames. Scale bar, 5 m.

Supplementary Figure 5

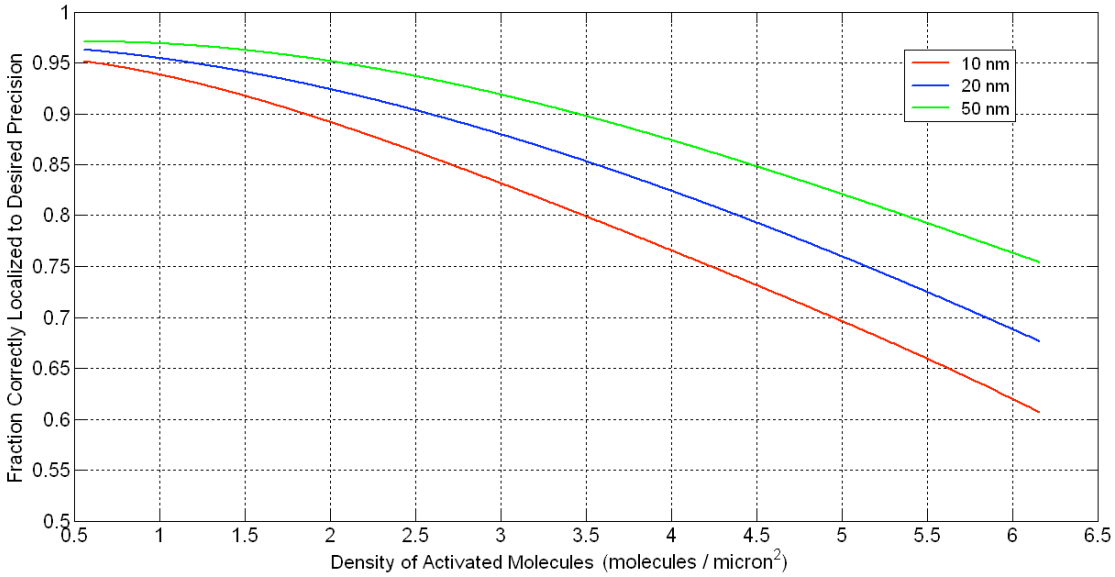

Localization precision vs. density of activated molecules in each frame of the PALM acquisition sequence. Curves represent the average of ten simulations at each of ten different densities, and show the fraction of randomly positioned molecules at each density that are correctly localized to each of three indicated levels of precision. Position estimates become increasingly inaccurate at higher activation densities as the diffraction-limited images of individual molecules increasingly overlap, setting a limit to the rate at which molecular information can be extracted from the sample.

Supplementary Figure 6

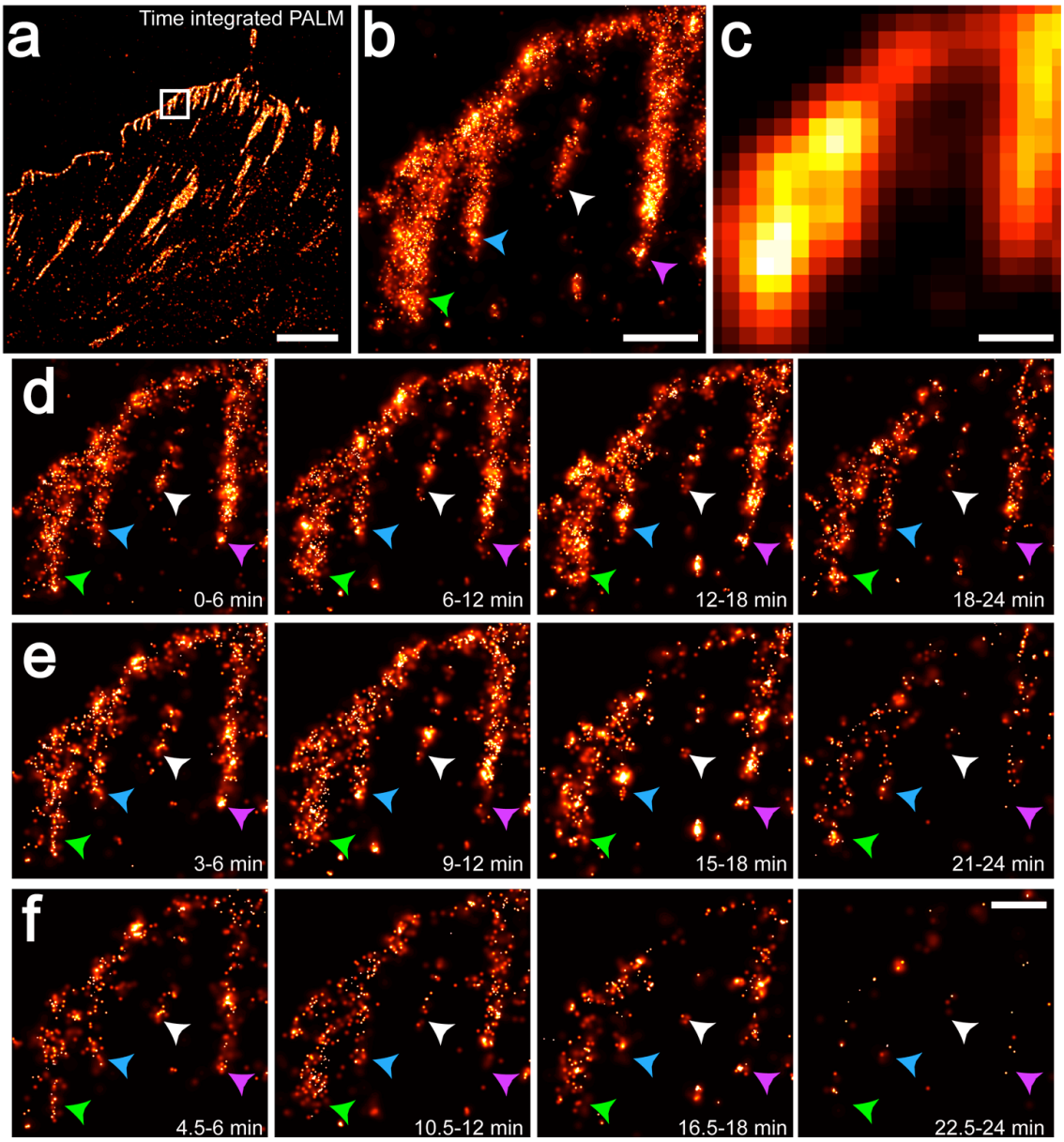

Stochastic molecular variations in fixed adhesion complexes. (**a**) Time integrated PALM image of a *fixed* CHO fibroblast expressing tdEos/paxillin. PALM-imaging was performed over 24 minutes, until all tdEos/paxillin molecules in the sample were bleached. The image is composed of 32,000 single-molecule frames. Scale bar, 5 m. (**b** and **c**) PALM and summed TIRF higher magnification views of the boxed area in (**a**). Smaller sub-ACs (blue, white arrowheads) are not resolved in the summed TIRF image. (**d, e, f**) Data in (**b**) are binned into four, eight, or 16 frames. ACs are progressively harder to resolve in later frames as molecules are bleached, and lower density ACs (blue, white arrowheads) are harder to resolve than higher density ACs (green, purple arrowheads). Stochastic variations in molecular density are more prominent, and resolution degrades, as the molecular budget/frame decreases. Scale bar in (**b**-**f**): 500 nm.

Supplementary Table 1.

Desired Resolution	Max Molecular Separation (nm)	Min Required Molecular Density	Min Molecules Required per DLR
50 nm (1D)	25	40 / m	10
20 nm (1D)	10	100 / m	25
10 nm (1D)	5	200 / m	50
50 nm (2D)	25	1.6×10^3 / m^2	80
20 nm (2D)	10	10^4 / m^2	500
10 nm (2D)	5	4×10^4 / m^2	2000
50 nm (3D)	25	6.4×10^4 / m^3	1600
20 nm (3D)	10	10^6 / m^3	2.5×10^4
10 nm (3D)	5	8×10^6 / m^3	2×10^5

Molecular Densities Required for Nyquist-Limited Resolution. The maximum molecular separation (2nd column) in each frame of a live cell PALM movie must be no more than half the desired resolution (1st column). Also shown are the corresponding minimum required molecular densities in 1, 2, and 3 dimensions (3rd column) and the minimum number of molecules per diffraction limited region (DLR, 4th column). Assumed DLRs were defined as follows: 1D, a line 250 nm in length; 2D, a circle with diameter 250 nm; 3D, a cylinder with height 500 nm and diameter 250 nm.

Supplementary Table 2.

Filter	Purpose	Location
FF562-Di02-25x36 (dichroic, Semrock)	Reflection of excitation, activation light; transmission of activated Eos fluorescence, DIC illumination	Filter cube in microscope body
NF01-568U-25 (notch filter, Semrock)	Additional suppression of excitation light	Filter cube in microscope body
565 dcxr (dichroic, Chroma)	Separation of activated Eos fluorescence from DIC illumination	Dual-Cam
FF01-617/73-25 (bandpass filter, Semrock)	Isolation of activated Eos fluorescence	Dual-Cam (fluorescence arm)
FF01-485/70-25 (bandpass filter, Semrock)	Isolation of DIC illumination	Dual-Cam (DIC arm)
21003a (linear polarizer, Chroma)	Analyzer for DIC	Dual-Cam (DIC arm)

Filters used in Olympus microscope and Photometrics Dual-Cam™.

Supplementary Discussion

Spatial Resolution, Signal to Noise, and Molecular Density. A number of criteria exist for quantifying resolution in microscopy. One classical measure, the Rayleigh criterion, is based on the minimum distance below which two point objects cannot be distinguished from one another, due to the overlap of their finite-sized, resolution-dictated images. However, most applications involve samples much more complex than pairs of points, and the ability to resolve such pairs does not necessarily imply the ability to resolve many features packed together at distances comparable to the Rayleigh limit. Furthermore, the Rayleigh criterion yields only a measure of the theoretically obtainable resolution, and not the image quality at that resolution or indeed at any other, coarser length scales at which features are resolvable.

Another, more comprehensive, measure uses the fact that any imaging system can be considered a spatial filter, which maps the sinusoidal Fourier components of the object onto an image, with differing degrees of fidelity based on the spatial frequency (e.g., line pairs / m) of each component. Typically, higher spatial frequencies are transmitted with increasingly poor contrast, and the theoretical resolution limit occurs at the spatial frequency f_{max} at which the contrast first drops to zero. Shot noise, background, and other noise sources limit the practical resolution even further, defining a non-zero limit to the contrast below which a weakly modulated spatial frequency cannot be detected. The plot of contrast vs. spatial frequency is known as the modulation transfer function (MTF). It yields not only the theoretical resolution, but also the quality with which the instrument can reproduce each spatial frequency in the final image.

A similar formulation can be adapted to PALM, even though the image represents an assemblage of discrete molecules rather than a continuum of labeled material. Clearly, no spatial frequency within the object can be observed in a PALM image unless the mean separation between neighboring molecules is sufficiently small to sample enough points per period at that frequency (**Fig. 1a**). Indeed, by analogy to the Nyquist criterion[1], the mean molecular separation must be smaller than half of the shortest detectable spatial period $T_{min} = 1/f_{max}$, hereby defined as the *Nyquist-limited* spatial resolution. For a *D*-dimensional image, T_{min} can then be related to the minimum required molecular density: $\rho \geq (2/T_{min})^D$, where ρ refers to the linear, areal, or volumetric density for $D = 1$, 2, or 3, respectively.

Even this standard represents more of a necessary than a sufficient condition, since it implies on average only one molecule per superresolution pixel of width $T_{min}/2$. Assuming equal probability that any given target molecule is labeled with a photoactivatable tag, and equal

probability that any such tag is photoactivated during a given PALM frame, the standard deviation in the number of molecules N per pixel is $\sigma_N = \sqrt{N}$. Thus, the Nyquist limit for PALM represents the spatial frequency at which the signal-to-noise ratio *SNR* drops to unity. This is the situation simulated in row 2, column 2 and row 3, column 3 of **Fig. 1a.**

In many cases, images of substantially higher *SNR* will be desired, as in **Fig. 1a**, row 2, columns 3, 4, and 5, which exhibit *SNR* = 2, 4, and 8, respectively. In such cases, $(SNR)^2$ molecules must be localized at each pixel, leading to a required molecular density of:

$$\rho \geq (SNR)^2 (2/\mathrm{T}_{\min})^D \tag{1}$$

from which we can define an *SNR-limited* resolution $\mathrm{T}(SNR)$ at a given molecular density:

$$\mathrm{T}(SNR) = 2\left(\frac{(SNR)^2}{\rho}\right)^{1/D} \tag{2}$$

or, alternatively, *SNR* as a function of the spatial frequency $f = 1/\mathrm{T}$:

$$SNR(f) = \sqrt{\rho / (2f)^D} \tag{3}$$

Log-log plots of $SNR(f)$, similar to traditional MTF plots, are shown for D = 1, 2, or 3 and various densities ρ in **Supplementary Fig. 1**. The minimum molecular densities required for various levels of Nyquist-limited resolution are given in **Supplementary Table 1**, as are the number of molecules on average in a diffraction limited region (DLR) at each of these densities.

Note that this relationship between molecular density and resolution is relevant to any microscope dependent upon discrete labeling, such as fluorescence microscopy. In particular, it highlights the importance of dense labeling to achieve a high Nyquist-defined resolution and/or high *SNR* in any form of superresolution fluorescence microscopy, such as near-field microscopy[2], stimulated emission depletion microscopy[3], or PALM[4]. Such dense labeling can be achieved with fluorescent protein fusions, but is much harder to obtain, particularly in the context of live cell imaging, using exogenously introduced labels such as dye conjugated antibodies.

Supplementary Methods

Sample Preparation

Glass coverslips were cleaned[5], then exposed to hexamethyldisazane (Sigma-Aldrich, 37,921-2) vapor at 120°C for 1 hr to enhance protein absorption. Cooled coverslips were coated overnight at 4°C with 5 g/ml fibronectin. NIH 3T3 cells were plated on the coverslips overnight before transfection with tdEOS/paxillin according to the method previously described[6]. CHO-K1 cells were grown on tissue culture plastic and transfected with tdEOS/paxillin using Lipofectamine LTX (Invitrogen) according to the manufacturer's protocol. The CHO-K1 cells were trypsinized and plated on the silanized fibronectin-coated coverslips and allowed to spread for approximately 2 hrs. Approximately 30 min before imaging, 100 nm diameter Au beads were added to the cells to serve as fiducials[5].

Equipment and Settings

With the exception of portions of **Fig. 2** and **Fig. 5** (as noted in the main text), all PALM images were rendered with the 'hot' colormap in *Matlab* that varies smoothly from black through shades of red, orange, and yellow to white. Details of the rendering algorithms are described in the supplementary material, section 6 of reference 4. Only those molecules that were localized to better than 30 nm were plotted in PALM images. **DIC images were processed using *Photoshop* (Adobe) with the *Fovea Pro* (Reindeer Graphics) "flatten surface" plug-in and a 50% difference Marr-Hilldreth filter with =0.4 and =0.6 pixels. The kymographs in Supplementary Figure 2 were made from DIC images using *ImageJ* (http://www.rsb.info.nih.gov/ij). The kymographs were collected from line scans orthogonal to a protrusive region of the cell.**

Supporting References

1**.** Shannon, C.E. Communication in the presence of noise. *Proc. IRE* **37**, 10-21 (1949).

2. Betzig, E. & Trautman, J.K. Near Field Optics: Microscopy, Spectroscopy, and Surface Modification Beyond the Diffraction Limit. *Science* **257**, 189-195 (1992).

3. Willig, K.I., Rizzoli, S.O., Westphal, V., Jahn, R., & Hell, S.W. STED microscopy reveals that synaptotagmin remains clustered after synaptic vesicle exocytosis. *Nature* **440**, 935-939 (2006).

4. Betzig, E. *et al*. Imaging Intracellular Fluorescent Proteins at Nanometer Resolution. *Science* **313**, 1642-1645 (2006).

5. Shroff, H. *et al*. Dual-color superresolution imaging of genetically expressed probes within individual adhesion complexes. *Proc. Natl. Acad. Sci. USA* **104**, 20308-20313 (2007).

6. Galbraith, C.G., Yamada, K.M., & Galbraith, J.A. Polymerizing Actin Fibers Position Integrins Primed to Probe for Adhesion Sites. *Science* **315**, 992-995 (2007).